Applied Catalysis B: Environmental 132–133 (2013) 39–44

Contents lists available at SciVerse ScienceDirect

Applied Catalysis B: Environmental

journal homepage: www.elsevier.com/locate/apcatb

Visible-light photocatalysis with phosphorus-doped titanium(IV) oxide particles prepared using a phosphide compound

Motoki Iwase[a], Keiji Yamada[a], Tsutomu Kurisaki[a], Orlando Omar Prieto-Mahaney[b], Bunsho Ohtani[b], Hisanobu Wakita[a,*]

[a] Department of Chemistry, Faculty of Science, Fukuoka University, 8-19-1 Nanakuma, Jonan-ku, Fukuoka 814-0180, Japan
[b] Catalysis Research Center, Hokkaido University, Kita-ku N21W10, Sapporo 001-0021, Japan

ARTICLE INFO

Article history:
Received 12 June 2012
Received in revised form 25 October 2012
Accepted 11 November 2012
Available online 23 November 2012

Keywords:
Titania
Phosphorus
Photocatalysis
Phosphorus-doped titania
Phosphide

ABSTRACT

Doping titanium(IV) oxide(TiO_2) with phosphorus (P) having negative charges was attempted in order to obtain P-doped TiO_2 with a red shift of the absorption edge and visible-light photocatalytic activity. P-doped TiO_2 was synthesized through the hydrolysis of titanium tetraisopropoxide in a suspension containing phosphide. The P-doped TiO_2 nanoparticles exhibited a pale yellow color. The UV–vis diffuse reflection spectra of P-doped TiO_2, which was calcined at 450–600 °C, showed a continuous and tailing absorption in the visible region. XRD patterns of P-doped TiO_2 showed the presence of anatase phase up to a temperature of 500 °C and the appearance of rutile phase from a temperature over 550 °C. The red shift of the absorption edge was not associated with the phase transformation from anatase to rutile. The XPS P2p spectra of P-doped TiO_2 indicated the decrease of P^{5+} and the increase of P^{3-} during sputtering. The results suggested the presence of phosphate on the surface and the presence of P^{3-} on the inner side of P-TiO_2. The action spectra of photocatalytic reaction for acetaldehyde decomposition revealed visible light activity of P-doped TiO_2. P-doped TiO_2 calcined at 475 °C was the most active in degradation of phenol under visible light. The P-content was found to play a key role in determining the spectral response in visible area and the photocatalytic activity under visible light irradiation.

1. Introduction

Titanium(IV) oxide (TiO_2) has been extensively used and investigated for the remediation of environmental organic pollutants because of the advantage of being a nontoxic, stable and inexpensive photocatalyst [1–3]. However, its wide band gap (3.2 eV for the anatase structure) allows it to absorb only ultraviolet light, which accounts for only ~6% of solar photons. A large number of approaches have been taken to reduce the band-gap energy of TiO_2 by doping with transition metal cations [4,5] and non-metal anions of elements such as N [6–16], C [17,18] and S [19,20]. N-doped TiO_2 has been synthesized by using NH_3 [6–9], urea [10–12], ethylenediamine [13], ethylmethylamine [14] or NH_4Cl [15,16] as a precursor of N. The properties of N-doped TiO_2 have already been discussed with respect to the nitrogen content [8], oxidative power [9], desorption of nitrogen from the O—Ti—O matrix in annealing [14], characterization of different prepared materials [15], increase of carrier-recombination centers in TiO_2 [11], and the effect of Fe_2O_3 nanoparticles on N-doped TiO_2 [12].

In general, phosphorous doped (P-doped) TiO_2 prepared using phosphate is not able to absorb visible light. Some groups [21–24] have reported that P-doped TiO_2 prepared using H_3PO_4 had a slight larger band gap than that of pure TiO_2. On the other hand, results of several experiments on P-doped TiO_2 prepared using phosphate with band gap narrowing (a red shift of the absorption edge) have been reported [25–28]. In those studies, P-doped TiO_2 was synthesized by a sol–gel method using $H_3PO_2(P^+)$ [25–27] or $H_3PO_4(P^{5+})$ [28] as a precursor of P. The band-gap energies of P-doped TiO_2 prepared using H_3PO_2 and H_3PO_4 were 3.13 eV (absorption edge: 396 nm) [26] and 3.11 eV (399 nm) [28], respectively. Those studies suggested formation of Ti—O—P bonds in the anatase lattice [27,28]. The P species in the titania were considered to be the dominant group responsive to the small change in band gap [27]. Yang et al. reported first-principles calculation for substitutional P-doped anatase and rutile TiO_2 [29]: in the case of doping anatase TiO_2 with phosphorus having positive charges and in the case of doping rutile TiO_2 with phosphorus, the band gaps of the doped TiO_2 had little narrowing. On the other hand, in the case of doping anatase TiO_2 with phosphorus having negative charges, the band gap of the doped TiO_2 had a slight narrowing because some P3p states were considered to exist in it. That study suggested that doping anatase TiO_2 with phosphorus having negative charges made it

* Corresponding author. Tel.: +81 92 801 8883; fax: +81 92 801 8883.
E-mail address: wakita@fukuoka-u.ac.jp (H. Wakita).

0926-3373/$ – see front matter © 2012 Elsevier B.V. All rights reserved.
http://dx.doi.org/10.1016/j.apcatb.2012.11.014

possible to prepare P-doped TiO_2 with visible-light photocatalytic activity.

We have reported the characterization of P-doped TiO_2 prepared by calcination after grinding phosphide (P^{3-}) and TiO_2 materials in a mortar [30]. However, a shift of the absorption edge was not apparent. A possible interpretation is that P species could not be sufficiently introduced into the TiO_2 lattice because phosphide and TiO_2 materials were mixed in solid form. The purpose of the present study was the first synthesis of P-doped TiO_2 with a red shift of the absorption edge and visible-light photocatalytic activity using a phosphide compound as a precursor of P. The mixing process of phosphide and TiO_2 materials was performed in solution. Visible-light activity was investigated using action spectra. The features of visible-light photocatalysis for P-doped TiO_2 are discussed.

2. Experimental

2.1. P-doped TiO_2 preparation

All chemicals used in this study except for a few obtained from companies shown in parentheses were purchased from Wako Pure Chemical Industries, Ltd.

P-TiO_2 was synthesized by calcination of the precipitates after hydrolysis of titanium tetraisopropoxide in a suspension containing phosphide. First, phosphide was synthesized as follows: Titanium tetrachloride was mixed with 2 equiv. of cyclohexylphosphine (Strem Chemicals Inc.) in hexane at ambient temperature. A pure yellow solid of $[TiCl_4(C_6H_{11}PH_2)_2]$ was separated by filtration [31]. After the yellow solid had been heated in an ampoule under nitrogen atmosphere at 450 °C for 6 h, a black solid (denoted as *TiP compound*) was obtained. Then the phosphide and TiO_2 materials were mixed as follows: 0.017 g of the *TiP compound* was dispersed in a mixture of 2.84 g titanium tetraisopropoxide and 6 mL 2-propanol. The following hydrolysis process was achieved by adding 30 mL of deionized water (Milli-Q water, Millipore) dropwise into the solution under stirring. A gray precipitate was produced instantly, and the mixture was stirred for 10 min. The precipitate was separated by filtration and washed 3 times with deionized water. The collected solids were dried at 110 °C for 3 h and calcined for 6 h at 450–600 °C. (These products are denoted as P-TiO_2(T), T: each calcination temperature.) P_{high}-TiO_2 was prepared in the same way with 10 times higher ratio of P. ST01 (Ishihara Sangyo Kaisha, Ltd.) was used as a reference. PO_4-adsorbed TiO_2 was prepared as follows: ST01 powder (1.0 g) was added to 100 mL aqueous H_3PO_4 solution (20 mM), and the solution was kept stirring for 1 h in dark. The PO_4-adsorbed TiO_2 powder was obtained after being filtered and dried at 110 °C for 3 h.

2.2. Characterization

The crystal structure of TiO_2 was examined by an X-ray diffraction method (XRD) using Rigaku Multiflex 2 kW with a Cu-Kα source. The chemical composition on the surface of TiO_2 was examined by X-ray photoelectron spectroscopy (XPS) using PHI model for 1800 equipped with a monochromatic Al-Kα source at a pass energy of 23.5 eV. The core level binding energies were aligned with respect to the C1s binding energy of 285 eV. An electron flood gun was used to compensate for the build-up of positive charge on the insulated samples during the measurement. Ar^+ sputtering (2 kV) was applied to examine the surface of the samples. UV–vis absorption spectra were recorded by a JASCO V-570 UV–vis spectrometer. The specific surface area of TiO_2 was analyzed by the BET method from N_2 adsorption isotherms at 77 K using BELSORP-max.

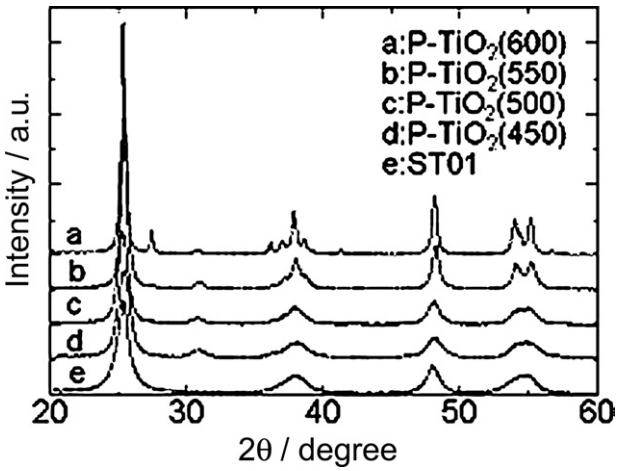

Fig. 1. XRD patterns of ST01 and P-TiO_2 at different calcination temperatures.

The samples were dried at 110 °C for 3 h before the adsorption measurement. IR spectra were investigated using JASCO FT/IR-480Plus.

2.3. Action spectra

Action spectra were measured with monochromatic light irradiation in the wavelength range from 350 nm to 470 nm using a diffraction grating-type illuminator (JASCO, CRM-FD) equipped with a 300-W Xenon lamp (Hamamatsu Photonics, C2578-02). The light intensity at each wavelength was detected by a power meter (HIOKI 3664). Full-width at half-maximum intensity (FWHM) of monochromatic light was ca.15 nm. A container containing the sample photocatalyst (10 mg) and acetaldehyde was sealed and kept in the dark for 2 h to reach an adsorption equilibrium. The molar amounts of CO_2 as a result of photocatalytic decomposition of acetaldehyde were measured by a gas chromatograph (Shimadzu, GC-14B) equipped with an FID and a methanizer (Shimadzu, MTN-1).

2.4. Photocatalytic activity measurements

The photocatalytic activity of P-TiO_2 was determined by measuring the degradation of phenol and the appearance of 1,4-benzoquinone under irradiation. Phenol is one of the model compounds for photocatalytic degradation [32]. An aqueous suspension (5.0 mL) of TiO_2 (8.0 g/L) and phenol (0.050 mM) was prepared. Irradiation was performed with a 450-W incandescent lamp (Iwasaki Electric Co. Ltd.). Wavelengths were selected with a Y-45 glass filter (AGC Techno Glass Co., Ltd.) and an aqueous nickel sulfate solution to emit in the 423–600 nm range. The suspensions were stirred for 15 min prior to and during the irradiation. After irradiation, samples were extracted through a 0.45 μm Sartorius filter (MINISART RC4) for analysis by HPLC (Shiseido Fine Chemicals, Nanospace system). Compounds were separated on a reversed-phase column (Shiseido Fine Chemicals, C18AQ) with H_3PO_4 buffer (0.1 wt.%)/CH_3OH (90:10). Photodiode array detection at 260 nm was used for quantification.

3. Results and discussion

3.1. Photocatalyst structure

First-principles calculation [29] predicted that crystal structure was an important factor for the preparation of P-TiO_2 with visible light photocatalytic activity. Fig. 1 shows XRD patterns of P-TiO_2 and ST01. The XRD patterns of P-TiO_2 up to a temperature of 500 °C

Table 1
Crystallite sizes and surface areas of P-TiO_2 and ST01.

Sample	Crystallite size (nm)	Surface area ($m^2\,g^{-1}$)
ST01	8.8	297
P-TiO_2(450)	8.1	127
P-TiO_2(500)	10	99
P-TiO_2(550)	18	56
P-TiO_2(600)	37	29

correspond to the pattern of ST01 which is in the anatase form. Rutile growth begins to appear at 550 °C. Small peaks around 31° indicate the existence of a small quantity of brookite crystal structure. The data are consistent with the results of a study [33] in which sol–gel synthesis of titania produced a mixture of brookite and anatase. Crystallite size was determined using Scherrer's equation [34]:

$$D = \frac{0.89\lambda}{\beta \cos \theta} \quad (1)$$

where λ (nm) is the X-ray wavelength, θ is the Bragg angle, and β is the corrected full width at half maximum (FWHM) of the most intense diffraction peak. The crystallite sizes for P-TiO_2 and ST01 are summarized in Table 1. The size of ST01 was 8.8 nm, comparable to the reported data [35]. The size for P-TiO_2 increased with increase in calcination temperature. The specific surface areas of P-TiO_2 and ST01 are also summarized in Table 1. The surface area of ST01 is in good agreement with the reported data [35]. The surface area of P-TiO_2 decreased with increasing calcination temperature.

3.2. UV–vis absorption spectra

Fig. 2(A) shows absorption spectra before and after calcination. The absorption in the range of 400–500 nm before calcination is attributed to the color of the *TiP compound* itself. The disappearance of absorption in the same range after calcination indicates the formation of a different state for P species.

Fig. 2(B) shows absorption spectra of P-TiO_2 and ST01. All of the synthesized P-TiO_2 samples exhibit a pale yellow color. The UV–vis spectra of P-TiO_2 show a continuous and tailing absorption in the visible region. The absorption edge around 400 nm for ST01 is assigned to electronic transitions from the valance band to conduction band for the anatase phase. The band-gap energies of P-TiO_2(500) and ST01 are 2.94 and 3.09 eV, respectively, which were determined by the plot of the modified Kubelka–Munk function $(ahv)^{1/2}$ versus photon energy assuming indirect transition. The spectra of P-TiO_2(500), which is in the anatase and brookite form, are clearly modified by the onset of a relatively broad absorption band in the visible region. The red shift of P-TiO_2 does not correlate with brookite phase because the band-gap energy of brookite is reported to be 3.14 eV [36]. The absorption spectra and XRD analysis of P-TiO_2 indicate that the red shift of the absorption edge is not associated with the phase transformation from anatase to rutile.

3.3. FTIR spectra

Fig. 3 shows FTIR spectra for P-TiO_2 and ST01. The signals in the range of 700–1250 cm^{-1} are characteristic of formation of the O—Ti—O lattice [15]. The infrared spectra of all samples show signals at 1630 cm^{-1}, 2340 cm^{-1} and 3400 cm^{-1}(broad), which are ascribed to OH [15], adsorbed CO_2 [16] and residual adsorbed water [16], respectively. The 1630 cm^{-1} and 3400 cm^{-1} peaks decrease with increasing calcination temperatures. A 1300 cm^{-1} signal, which is characteristic of C—H [14], was not detected. Zhao et al. reported that the signals for organic groups of the raw material

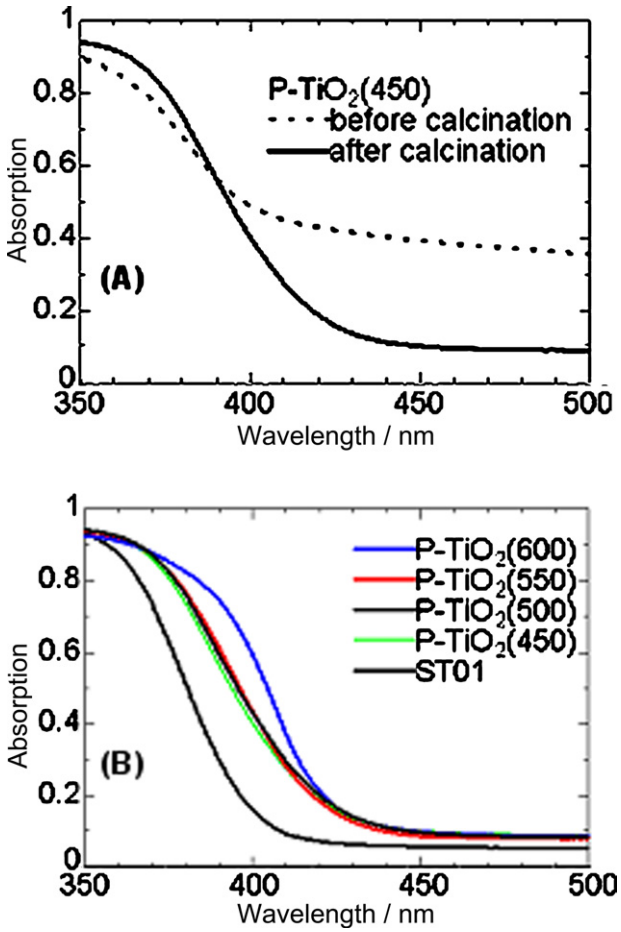

Fig. 2. Absorption spectra of P-TiO_2(450) before calcination and after calcination (A) and absorption spectra of ST01 and P-TiO_2 at different calcination temperatures (B).

in IR spectra disappeared with heating at 400 °C for 30 min in their process for synthesis of TiO_2 [13]. Since P-TiO_2 was calcined at a temperature above 400 °C for 6 h, no peak corresponding to hydrocarbon can be seen in Fig. 3. A 1030 cm^{-1} peak, which corresponds to PO_4 [37], was not observed in our calcination process despite partial oxidation of P on the surface (see Fig. 4). This suggests that a small quantity of P atoms exists on the surface of TiO_2 (see Table 2).

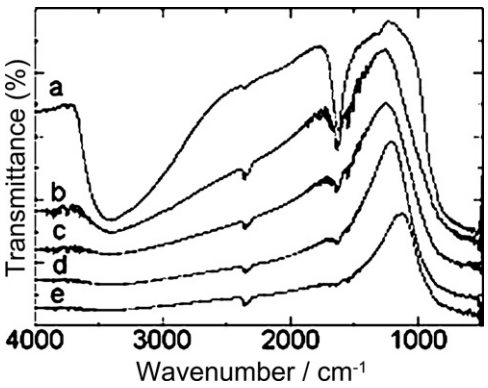

Fig. 3. IR spectra of ST01 (a), P-TiO_2(450) (b), P-TiO_2(500) (c), P-TiO_2(550) (d), and P-TiO_2(600) (e).

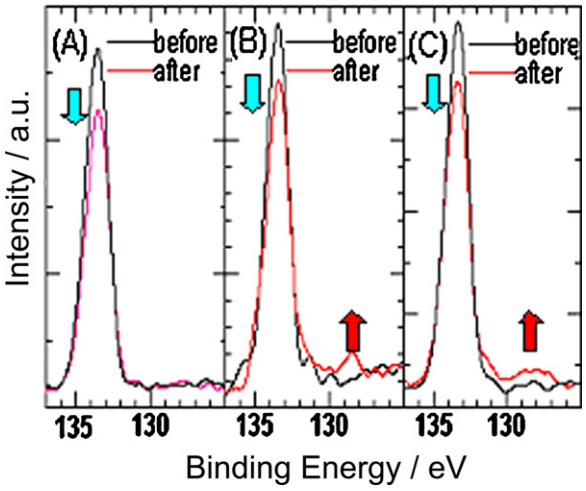

Fig. 4. XPS P2p spectra of PO_4-adsorbed TiO_2 (A), P-TiO_2(500) (B), and P_{high}-TiO_2 (C) before and after sputtering.

3.4. XPS analysis

Fig. 4 shows P2p spectra of P-TiO_2, P_{high}-TiO_2, and PO_4-adsorbed TiO_2 before and after sputtering. A peak at 134 eV is assigned to P^{5+} [22]. The decrease of the peak intensity for PO_4-adsorbed TiO_2 during sputtering in Fig. 4(A) indicates the presence of phosphate on the surface of TiO_2. The same behaviors of the peaks at 134 eV were observed for P-TiO_2 and P_{high}-TiO_2 in Fig. 4(B and C). These results indicate the presence of phosphate on the surface of P-TiO_2 and P_{high}-TiO_2 resulted from the partial oxidation of phosphide during our synthetic process. A peak at approximately 128 eV is assigned to P^{3-} [22]. The increase of the peak intensities at 128 eV for P-TiO_2 and P_{high}-TiO_2 during sputtering indicates the presence of P^{3-} on the inner side of TiO_2. Furthermore, the color change from gray to pale yellow during calcination as shown in Fig. 2(A) indicates the formation of different states for phosphorus atoms because gray is attributed to the *TiP compound* of raw materials. Theoretical calculation [29] predicted that visible light absorption of P-TiO_2 required the replacement of O atoms by P atoms having negative charges in the TiO_2 anatase matrix. Thus, the detection of P^{3-} in P-TiO_2, color change and theoretical calculation suggest that the dopant P is located at a substitutional site for an O atom in the anatase TiO_2 crystal. The red shift of the absorption edge of P-TiO_2 is interpreted as band gap narrowing induced by P^{3-} atoms in the TiO_2 anatase matrix.

The surface composition of P-TiO_2 was calculated using the sensitivity coefficient from peak areas of the XPS analysis. The composition is summarized in Table 2. The value of P/Ti for P-TiO_2(600) is larger than those for P-TiO_2(450, 500, 550). Nitrogen-content of nitrogen-doped TiO_2 usually decreased with the enhanced calcination temperature because of desorption of nitrogen from the O—Ti—O matrix in annealing [13]. The behavior of P-content on the surface of P-TiO_2 was found to be different from that of

Table 2
Surface composition of P-TiO_2.

Sample	Ti (%)	P (%)	P/Ti[a] (XPS)	P/Ti[b] (wash)
P-TiO_2(450)	30.1	0.54	0.018	0.018
P-TiO_2(500)	29.4	0.53	0.018	0.019
P-TiO_2(550)	30.5	0.55	0.018	0.020
P-TiO_2(600)	30.6	1.02	0.033	0.035

[a] The values were calculated using XPS data.
[b] The values were obtained as follows: an aqueous suspension (100 mL) containing P-TiO_2(50 mg) was stirred for 1 h. Next, the TiO_2 particles were separated by filtration. Then the values of washed P-TiO_2 were calculated using XPS data.

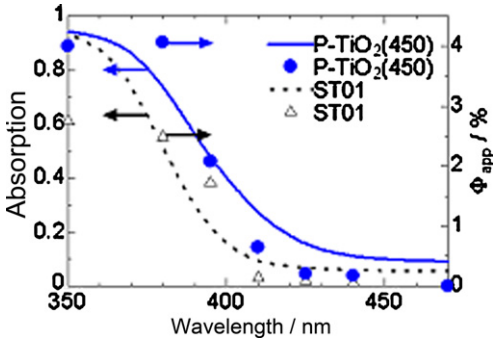

Fig. 5. Absorption and action spectra of P-TiO_2(450) (bold line and •) and ST01 (dotted line and Δ).

N-content on the surface of N-doped TiO_2. The values of P/Ti in P-TiO_2 after washing with water were also investigated by XPS analysis. Livraghi et al. [15] reported that the intensity of the N1s XPS peaks around 399–400 eV of nitrogen-doped TiO_2 prepared by a sol–gel method decreased and, in some cases, disappeared after washing with water in an ultrasonic bath. The values of P/Ti for P-TiO_2 after washing for 1 h (Table 2) are close to those of P/Ti before washing. The phosphorus atoms on the surface of P-TiO_2 were not eliminated by water.

3.5. Action spectra of acetaldehyde degradation

Action spectra were analyzed in order to investigate the wavelength range with visible-light photocatalytic activity. Fig. 5 shows the action spectra of photocatalytic reaction for acetaldehyde decomposition.

$$CH_3CHO + 5/2O_2 \rightarrow 2CO_2 + 2H_2O \quad (2)$$

Assuming that the formation of a molecule of CO_2 requires five pairs of e^- and h^+, the apparent quantum efficiency Φ_{app} was calculated as a ratio of the molar rate of the CO_2 generation to the flux of incident photons [38–40]. The apparent quantum efficiency was also calculated as a product of efficiencies of photoabsorption and electron–positive hole utilization [39]. Since the action spectra of P-TiO_2 corresponded well with the optical absorption spectra, the apparent quantum efficiency for acetaldehyde decomposition by use of P-TiO_2 was found to depend on the efficiency of photoabsorption. The apparent quantum efficiency of P-TiO_2 in Fig. 5 is ~0.66% in the 410–440 nm wavelength range, while the efficiency of ST01 falls to negligible values in the same wavelength range. These results show that the action spectra reveal the visible light photocatalytic activity of P-TiO_2. The apparent quantum efficiency of P-TiO_2 at the wavelengths longer than 420 nm appears to be low compared to its absorption spectra. In the absorption spectrum of P-TiO_2, broad (flat) absorption, without giving photocatalytic activity, might be overlapped to the absorption due to P-doping, which is responsible for activity. This led to apparent blue shift of an action spectrum from the absorption spectrum. It is also noted that the UV light activity of P-TiO_2 is larger than that of ST01. Previous studies on nitrogen-doped TiO_2 with visible-light activity showed that the photocatalytic efficiency of N-doped TiO_2 under UV light was less than that of pure TiO_2 [11,41]. The possible reason for the decrease in UV-light activity is that the N-doping causes formation of defect sites that lead to a loss of crystallinity [41] or that the N-doping causes an increase of carrier-recombination centers in TiO_2 [11].

3.6. Photocatalytic degradation of phenol

Fig. 6 shows the photodegradation of phenol (A) and the appearance of 1,4-benzoquinone (B) in the presence of P-TiO_2

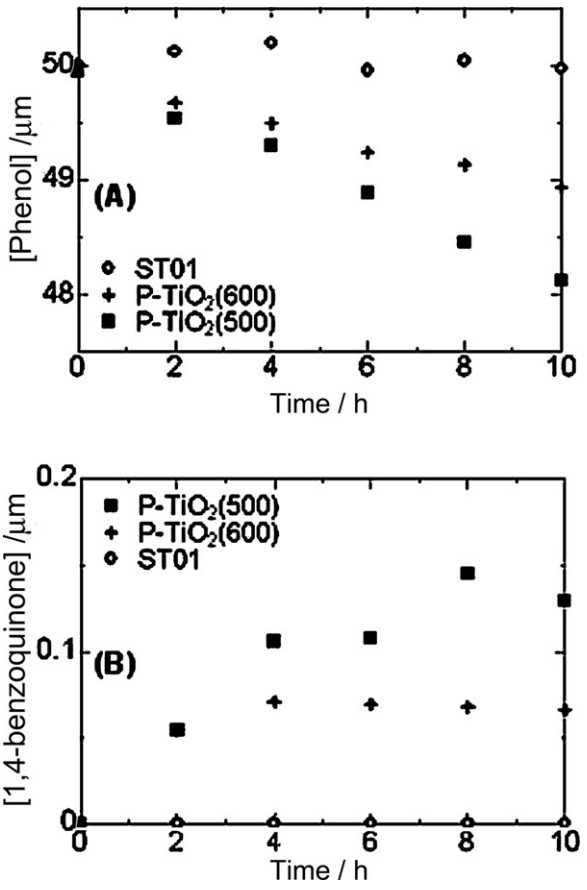

Fig. 6. Phenol degradation (A) and 1,4-benzoquinone formation (B) on P-TiO_2 and ST01 under visible light irradiation as a function of irradiation time.

and ST01 under visible light irradiation as a function of irradiation time. There was no degradation of phenol (A) or appearance of 1,4-benzoquinone (B) in the case of ST01 under visible light (423–600 nm) irradiation. On the other hand, the data for P-TiO_2 clearly show a decrease of phenol (A) and an increase of 1,4-benzoquinone (B). The experimental results indicate visible light activity of P-TiO_2 for phenol decomposition.

Fig. 7 shows apparent pseudo-first-order rate constants k_{app} for the photodegradation of phenol in the presence of P-TiO_2 as a function of calcination temperature. Up to a calcination temperature of 475 °C, the k_{app} value increases with increasing calcination temperature. On the other hand, the value above 475 °C decreases with increasing calcination temperature.

A large specific surface area causes a large amount of substrates to be adsorbed on TiO_2. Large specific surface areas are responsible

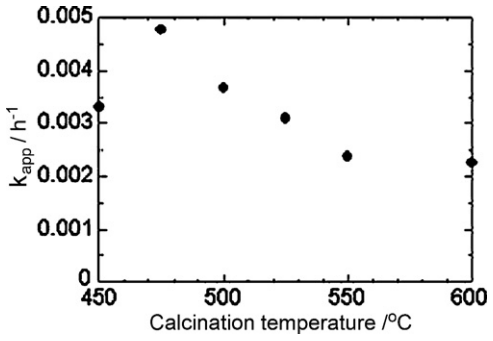

Fig. 7. Apparent rate constants k_{app} for photodegradation of phenol in the presence of P-TiO_2 as a function of calcination temperature.

for high photocatalytic efficiency [42]. In the present study, the specific surface area decreased with increasing calcination temperature as shown in Table 1. The large specific surface area in the range of 450–500 °C was associated with high photocatalytic efficiency at 475 °C.

3.7. Features of P-doped TiO_2

As for XPS analysis, a P2p peak of P-doped TiO_2 prepared using H_3PO_2 was observed around 132.6 eV [25]. In the present study, the peaks of P-TiO_2 were located around 134 eV (P^{5+}) and 128 eV (P^{3-}). The shape of absorbance for P-doped TiO_2 prepared using H_3PO_2 [26,27] was obviously different from that for P-TiO_2. The differences show that the properties of P-TiO_2 are not consistent with those of P-doped TiO_2 prepared using H_3PO_2. In the case of P/Ti in the range of 0.01–0.02, the absorption edges of P-TiO_2 and P-doped TiO_2 prepared using H_3PO_4 (P^{5+}) [28] and H_3PO_2 (P^+) [26] were 422, 399 and 396 nm, respectively. The trend corresponds to the first-principles calculation [29]. The calculation indicated that the band gap of the doped TiO_2 had a slight narrowing for P anion-doped TiO_2(anatase) which is prepared by replacement of lattice O^{2-} by P^{3-} and little narrowing for P cation-doped TiO_2 which is prepared by replacement of lattice Ti^{4+} by P^{5+}.

The difficulty for doping TiO_2 with phosphorus having negative charges is that P species cannot be easily introduced into the TiO_2 lattice. Preparation by mixing phosphide and TiO_2 materials in solution provided definitive evidence of a red shift in the absorption edge for P-TiO_2. The dispersion of phosphide before calcination was found to be an important factor for the preparation of P-TiO_2.

During preparation of P-TiO_2, replacement of O^{2-} by P^{3-} produces oxygen vacancies. In order to maintain the overall electroneutrality of the crystal lattice, incorporation of two P atoms into the oxygen sites causes formation of one oxygen vacancy. Hydrogen-reduced TiO_2 powders were known as an example of having a large quantity of oxygen vacancies [7]. The powder exhibited a gray color, which indicates absorption over the entire range of visible light. Because the UV–vis spectra of P-TiO_2 show a continuous and tailing absorption below 500 nm, a small amount of oxygen vacancies in P-TiO_2 does not have much influence on the absorption. Incidentally, the oxygen vacancy state is not visible-light sensitive because hydrogen-reduced TiO_2 powders were not visible-light sensitive [7]. However, the oxygen vacancy is thought to act as a recombination center for holes and electrons because the oxygen vacancy state in anatase TiO_2 is below the lower end of conduction band at 0.75–1.18 eV [43]. Doping TiO_2 with an excess amount of P leads to a considerable decrease of photocatalytic activity for P-TiO_2. Further investigation to find an optimal doping amount of P is in progress.

4. Conclusions

Doping anatase TiO_2 with phosphorus having negative charges results in the preparation of P-doped TiO_2 with a definite red shift of the absorption edge and efficient visible-light photocatalytic activity. The dispersion of phosphide before calcination was found to be an important factor for the preparation of P-TiO_2. The absorption edge of P-TiO_2 was obviously larger than that of P-doped TiO_2 prepared using H_3PO_4(P^{5+}) and H_3PO_2(P^+). The results are in agreement with the first-principles calculation for P anion-doped TiO_2. The action spectra of photocatalytic reaction for acetaldehyde decomposition proved the visible-light photocatalytic activity of P-TiO_2. The present study indicates that P^{3-}-doped TiO_2 should be investigated as a new material of nonmetal-doped TiO_2 that can yield clear reactivity under visible light.

Acknowledgments

The authors thank Dr. Kosei Shioji for the use of the visible-light lamp, Prof. Satoshi Kawata for the XRD measurement, Dr. Yoshio Murata for the reflectance spectrometer and Prof. Toshio Yamaguchi for assistance in the surface area analysis and IR experiment. Dr. Shioji, prof. Kawata, Dr. Murata and prof. Yamaguchi are all affiliated with Fukuoka University. This study was supported by the Cooperative Research Program of Catalysis Research Center, Hokkaido University (Grant #10B1013). This work was partly supported by Grant-in-Aid for Scientific Research (B) (20350040) and (C) (22550088).

References

[1] M.R. Hoffmann, S.T. Martin, W.Y. Choi, D.W. Bahnemann, Chemical Reviews 95 (1995) 69–96.
[2] T.L. Thompson, J.T. Yates Jr., Chemical Reviews 106 (2006) 4428–4453.
[3] B. Ohtani, Journal of Photochemistry and Photobiology C: Photochemistry Review 11 (2010) 157–178.
[4] M. Anpo, Y. Ichihashi, M. Takeuchi, H. Yamashita, Research on Chemical Intermediates 24 (1998) 143–149.
[5] A. Zielinska, E. Kowalska, J.W. Sobczak, I. Lacka, M. Gazda, B. Ohtani, J. Hupka, A. Zaleska, Separation and Purification Technology 72 (2010) 309–318.
[6] R. Asahi, T. Morikawa, T. Ohwaki, K. Aoki, Y. Taga, Science 293 (2001) 269–271.
[7] H. Irie, Y. Watanabe, K. Hashimoto, Journal of Physical Chemistry B 107 (2003) 5483–5486.
[8] T. Matsumoto, Y. Hashimoto, M. Sakai, W. Shimizu, T. Nishikawa, Y. Murakami, N. Iyi, B. Ohtani, Topics in Catalysis 52 (2009) 1584–1591.
[9] M. Mrowetz, W. Balcerski, A.J. Colussi, M.R. Hoffmann, Journal of Physical Chemistry B 108 (2004) 17269–17273.
[10] E.A. Reyes-Garcia, Y. Sun, K. Reyes-Gil, D. Raftery, Journal of Physical Chemistry C 111 (2007) 2738–2748.
[11] F. Amano, R. Abe, B. Ohtani, Transactions of the Materials and Research Society of Japan 33 (2008) 173–176.
[12] K. Nishijima, B. Ohtani, X. Yan, T. Kamai, T. Chiyoda, T. Tsubota, N. Murakami, T. Ohno, Chemical Physics 339 (2007) 64–72.
[13] Y. Zhao, X. Qiu, C. Burda, Chemical Materials 20 (2008) 2629–2636.
[14] T.C. Jagadale, S.P. Takale, R.S. Sonawane, H.M. Joshi, S.I. Patil, B.B. Kale, S.B. Ogale, Journal of Physical Chemistry C 112 (2008) 14595–14602.
[15] S. Livraghi, M.R. Chierotti, E. Giamello, G. Magnacca, M.C. Paganini, G. Cappelletti, C.L. Bianchi, Journal of Physical Chemistry C 112 (2008) 17244–17252.
[16] C.D. Valentin, G. Pacchioni, A. Selloni, S. Livraghi, E. Giamello, Journal of Physical Chemistry B 109 (2005) 11414–11419.
[17] S.U.M. Khan, M. Al-Shahry, W.B. Ingler Jr., Science 297 (2002) 2243–2245.
[18] B. Neumann, P. Bogdanoff, H. Tributsch, S. Sakthivel, H. Kisch, Journal of Physical Chemistry B 109 (2005) 16579–16586.
[19] Y. Izumi, T. Itoi, S. Peng, K. Oka, Y. Shibata, Journal of Physical Chemistry C 113 (2009) 6706–6718.
[20] X. Tang, D. Li, Journal of Physical Chemistry C 112 (2008) 5405–5409.
[21] L. Korosi, I. Dekany, Colloids and Surfaces A: Physicochem Engineering Aspects 280 (2006) 146–154.
[22] J.C. Yu, L. Zhang, Z. Zheng, J. Zhao, Chemical Materials 15 (2003) 2280–2286.
[23] Y. Lv, L. Yu, H. Huang, H. Liu, Y. Feng, Journal of Alloys and Compounds 488 (2009) 314–319.
[24] L. Korosi, S. Papp, I. Bertoti, I. Dekany, Chemical Materials 19 (2007) 4811–4819.
[25] L. Lin, Y. Zhu, B. Zhao, Y. Xie, Chemistry Letters 34 (2005) 284–285.
[26] L. Lin, W. Lin, J.L. Xie, Y.X. Zhu, B.Y. Zhao, Y.C. Xie, Applied Catalysis B 75 (2007) 52–58.
[27] R. Zheng, L. Lin, J. Xie, Y. Zhu, Y. Xie, Journal of Physical Chemistry C 112 (2008) 15502–15509.
[28] F. Li, Y. Jiang, M. Xia, M. Sun, B. Xue, D. Lin, X. Zhang, Journal of Physical Chemistry C 113 (2009) 18134–18141.
[29] K. Yang, Y. Dai, B. Huang, Journal of Physical Chemistry C 111 (2007) 18985–18994.
[30] M. Iwase, Y. Fujio, S. Nagahama, K. Yamada, T. Kurisaki, H. Wakita, Advances in X-ray Chemical Analysis, Japan 42 (2011) 213–219.
[31] T.S. Lewkebandara, J.W. Proscia, C.H. Winter, Chemical Materials 7 (1995) 1053–1054.
[32] S.T. Martin, C.L. Morrison, M.R. Hoffmann, Journal of Physical Chemistry 98 (1994) 13695–13704.
[33] S.L. Isley, R.L. Penn, Journal of Physical Chemistry B 110 (2006) 15134–15139.
[34] H.P. Klug, L.E. Alexander, X-ray Diffraction Procedure, John Wiley & Sons Inc., New York, 1954.
[35] Y. Nosaka, M. Matsushita, J. Nishino, A.Y. Nosaka, Science and Technology of Advanced Materials 6 (2005) 143–148.
[36] M. Graetel, F. Rotzinger, Chemical Physics Letters 118 (1985) 474–477.
[37] Y. Arai, D.L. Sparks, Journal of Colloids and Interface Science 241 (2001) 317–326.
[38] T. Torimoto, Y. Aburakawa, Y. Kawahara, S. Ikeda, B. Ohtani, Chemical Physics Letters 392 (2004) 220–224.
[39] B. Ohtani, Chemistry Letters 37 (2008) 217–229.
[40] M.V. Dozzi, B. Ohtani, E. Selli, Physical Chemistry Chemical Physics 13 (2011) 18217–18227.
[41] W. Balcerski, S.Y. Ryu, M.R. Hoffmann, Journal of Physical Chemistry C 111 (2007) 15357–15362.
[42] G. Tian, H. Fu, L. Jing, B. Xin, K. Pan, Journal of Physical Chemistry C 112 (2008) 3083–3089.
[43] I. Nakamura, N. Negishi, S. Katsuna, T. Ihara, S. Sugihara, K. Takeuchi, Journal of Molecular Catalysis A: Chemical 161 (2000) 205–212.